MODELING OF CREEP, SHRINKAGE AND TEMPERATURE EFFECTS IN INTEGRAL ABUTMENT BRIDGES

M. Sivakumar, Graduate Research Assistant, Florida Atlantic University, Boca Raton, FL
M. Arockiasamy, Ph.D., PE, Professor and Director, Center for Infrastructure and Constructed Facilities, Department of Civil Engineering, Florida Atlantic University, Boca Raton, FL

ABSTRACT

Superstructure of integral abutment bridges, which do not have joints either at abutment or at intermediate supports, is subjected to secondary stresses due to creep, shrinkage and thermal effects. Number of transportation agencies is using integral abutment concept, and they extend the maximum bridge length based on their experience. Although the stress levels generated by secondary effects are well-understood and advance the-state-of-the-art through experience, these effects are not well quantified. This study focuses on developing an analytical model and numerical procedure to predict instantaneous linear behavior and non-linear time dependent long-term behavior of uncracked and cracked composite superstructure used in integral abutment bridges due to long-term creep and shrinkage effects. The effect of fully continuos deck slab is incorporated in the model. The model includes the effects of creep, shrinkage, and cracking of concrete slab of composite steel/concrete girder bridges. The variations in the material property of the cross-section corresponding to the constituent material that are used in the structure are incorporated by transformed area of the cross-section. Creep and shrinkage are evaluated using the ACI model. Variation in concrete property with age is included using age-adjusted effective modulus. The model is used to analyze a two-span integral abutment bridge in which composite girder is used as superstructure. Partial rigidity provided by the substructure system is included in the analysis by modeling the abutment-wingwall-pile substructure system as discrete springs for translational and rotational degrees of freedom. The forces obtained from the analysis are used to determine and evaluate the response of laterally loaded piles that support the abutment.

Key words: Integral Abutment, Creep, Shrinkage, Substructure Stiffness, Laterally Loaded Piles

INTRODUCTION

Integral construction is used to avoid problems associated with bridge deck joints and reduce the construction and the maintenance costs. Continuous jointless deck integrally connected to the abutment is one of the major types of construction of integral abutment bridges. Integral abutment bridges accommodate superstructure movements without conventional expansion joints. One of the advantages of integral construction is better seismic resistance due to the added redundancy. The integral bridges differ from regular rigid frame bridges in the manner of distribution of stresses due to temperature change, prestressing, creep, shrinkage, and restraints provided by abutment foundation and backfill. Effects of connections at integral abutments are relatively complex and are not well understood. Continuity between the abutment and the superstructure results in secondary stresses. Time-dependent effects of creep, shrinkage and temperature on composite superstructure, passive pressure on integral abutments and pressure developed at abutment-pavement joint are main parameters governing the design. The behavior of integral abutment bridges is also influenced by the superstructure-substructure stiffness, type of foundation, connection details between the foundation and abutment, soil properties and soil settlement, and the connection between the approach slab and the deck system. Since only very limited design and construction specifications are available in the American Association of State Highway Transportation Officials' Specification for Highway Bridges (AASHTO, 1994), wide variations are found among various states in idealizing integral abutment bridges for analysis and design[1, 2]. Tennessee DOT has considerable experience in integral abutment bridge construction and do not perform any analysis for concrete superstructure bridges up to 800 ft in length[3]. Although the majority of the bridges with integral abutments perform adequately, many of them operate at high stress levels[4].

A detailed literature review revealed that, number of transportation agencies is using integral abutment concept, and they extend the maximum bridge length based on their experience. Although the stress levels generated by secondary effects are well understood from the field observations and performance, and advance the-state-of-the-art through experience, these effects are not well quantified. Design practices and assumptions relating to thermal effects, soil pressures, analysis of piles, creep and shrinkage effects, vary considerably among the agencies. Design and construction practices are based largely on past local experience and thus empirical in nature. This paper attempts to quantify theses effects through an analytical model to ensure efficient and reliable design and gives a rationale for the adoption of integral abutment bridges. An analytical procedure incorporating the time dependent behavior of the superstructure will aid in getting the appropriate forces transmitted to the substructure system of the integral abutment bridge rather than assuming the superstructure system and substructure as separate systems. When the superstructure consisting of concrete/steel girders and concrete deck slab is subjected to sustained service loads, it undergoes nonlinear time-dependent deformations in the concrete due to creep and shrinkage in addition to nonlinearity produced by cracking of the concrete. Though the effects of creep and shrinkage in a composite girder were investigated on continuous concrete bridges with simple supports [5,6,7], a detailed procedure to analyze integral abutment bridge is not available. A parametric study using two dimensional frame analysis was reported [8] on the effects of the superstructure and substructure stiffness. The stiffness of substructure system includes the contribution from abutment walls, pile foundation and soil [9]. This has been achieved by modeling the system as discrete spring stiffness for translational and rotational degrees of freedom.

THEORETICAL MODEL

In the present study, an analytical model to predict the time-dependent behavior of a two span continuous steel/concrete composite girder bridge with fixed end condition is presented. Concrete creep and shrinkage are evaluated using the ACI model. Variation in concrete property with age is included using age-adjusted effective modulus. The variation in the material properties across the depth of the cross section is accounted for by transformed area of the cross section. The short-term stress-strain relationship for concrete is linear elastic in compression and tension prior to cracking. Tension in concrete is neglected after cracking. The stress-strain relationship for steel in both compression and tension is assumed linear elastic. The strain distribution on any section at any time is assumed linear.

INSTANTANEOUS ANALYSIS

The instantaneous strain ε_{ai} at any point a on the section at a distance y below the top surface is defined in terms of top fiber strain ε_{oi} and the initial curvature k_i (Fig. 1 c)

$$\varepsilon_{ai} = \varepsilon_{oi} - yk_i \quad (1)$$

If the concrete under short-term load is assumed linear elastic, the initial stress distribution is

$$\sigma_{ai} = E_c \varepsilon_{ai}$$

$$\sigma_{ai} = E_c\left(\varepsilon_{oi} - yk_i\right) \quad (2)$$

The resultant initial axial force N_i is found by integrating the stress block over the depth of the section. In general

$$N_i = \int \sigma_i dA$$

$$N_i = E_c \varepsilon_{oi} A - E_c k_i B \quad (3)$$

where $A = \int dA$ = area of transformed cross section,

$$A = \sum_{j=1}^{m1} n_{cj} A_{cj} + \sum_{j=1}^{m2} n_{sj} A_{sj} \quad (4)$$

where A = equivalent cross sectional area
n_{cj} = modular ratio of j^{th} concrete layer = E_{cj} / E_{c1}
n_{sj} = modular ratio of j^{th} steel layer = E_{sj} / E_{c1}
A_{cj} = cross sectional area of j^{th} concrete layer
A_{sj} = cross sectional area of j^{th} steel layer
m_1 = number of concrete layers in the cross section
m_2 = number of steel layers in the cross section
E_{cj} = modulus of elasticity of j^{th} concrete layer

E_{sj} = modulus of elasticity of j^{th} steel layer
E_{c1} = modulus of elasticity of deck slab concrete layer (reference layer)

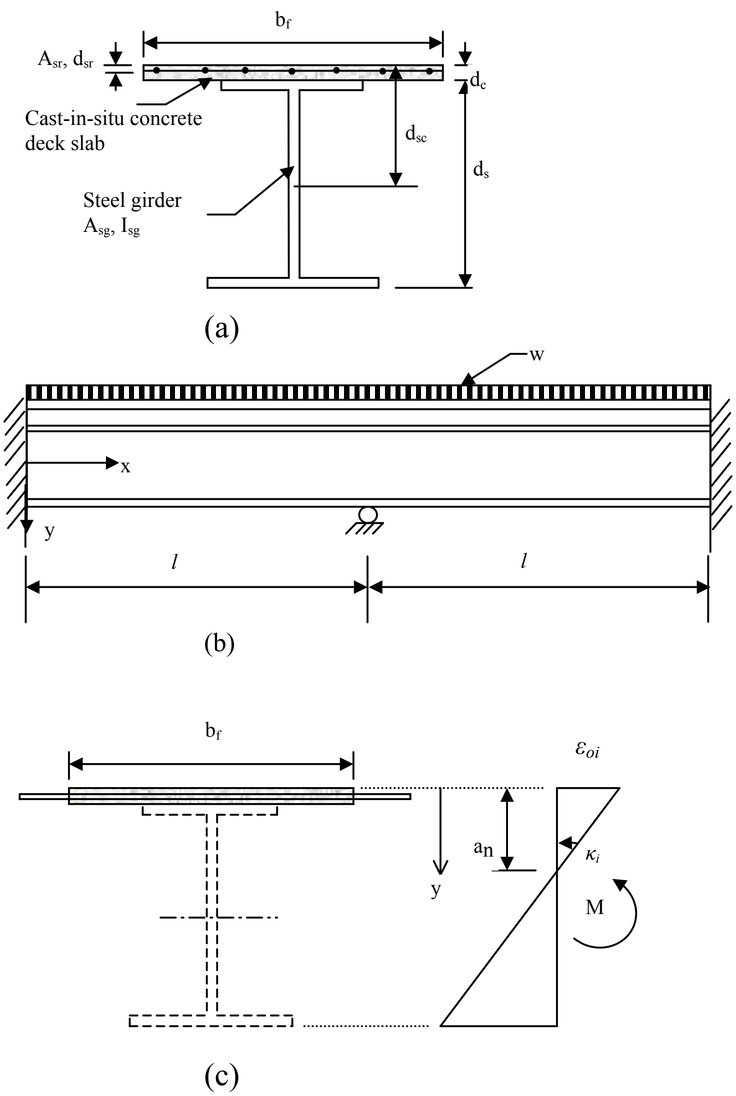

Fig.1 Details of Composite Integral Abutment Bridge System: (a) Cross Section; (b) Elevation; (c) Transformed Section and Strain Diagram

$B = \int ydA$ = first moment of transformed area about top fiber

$$B = \sum_{j=1}^{m1} n_{cj} A_{cj} d_{cj} + \sum_{j=1}^{m2} n_{sj} A_{sj} d_{sj} \qquad (5)$$

B = first moment of the transformed area about top fiber
d_{cj} = centroidal distance of j^{th} concrete layer from top fiber
d_{sj} = centroidal distance of j^{th} steel layer from top fiber

The initial bending moment about the top surface M_i is determined by integrating the first moment of the stress block about the top reference line.

$$M_i = -\int \sigma_i y dA$$

$$M_i = -E_c \varepsilon_{oi} B + E_c k_i I \quad (6)$$

where $I = \int y^2 dA$ = the second moment of the transformed section about the top surface of the section.

$$I = \sum_{j=1}^{m1} n_{cj} A_{cj} d_{cj}^2 + \sum_{j=1}^{m2} n_{sj} A_{sj} d_{sj}^2 \quad (7)$$

For any applied moment and axial force, the short-term strain distribution is obtained from

$$\begin{Bmatrix} \varepsilon_{oi} \\ k_i \end{Bmatrix} = \frac{1}{E_c\left(AI - B^2\right)} \begin{bmatrix} I & B \\ B & A \end{bmatrix} \begin{Bmatrix} N_i \\ M_i \end{Bmatrix} \quad (8)$$

Once the initial strain ε_{oi} and curvature, k_i are found from the transformed cross section, stress across the depth of the composite section for short-term analysis will be

$$\sigma_{cij} = E_{cj}\left(\varepsilon_{oi} - d_{cj} k_i\right) \quad (9)$$

$$\sigma_{sij} = E_{sj}\left(\varepsilon_{oi} - d_{sj} k_i\right) \quad (10)$$

where σ_{cij} = instantaneous stress at j^{th} layer of concrete
σ_{sij} = instantaneous stress at j^{th} layer of steel

If the stress in the concrete at the hogging bending moment region exceeds the tensile strength of the concrete f_t', the concrete is no longer effective and contribution of concrete to the transformed area is ignored.

TIME DEPENDENT ANALYSIS INCLUDING CREEP AND SHRINKAGE

During any time interval, the strain state is frozen, i.e., the strain distribution is assumed to remain unchanged in the relaxation procedure. If the total strain is held constant and the creep and shrinkage components change, then the instantaneous component of strain must also change by an equal and opposite amount. When the instantaneous strain changes, the concrete stress also changes. The stress on the cross section is, therefore, allowed to vary freely due to relaxation. Consequently, the internal actions change and equilibrium is not maintained. To restore equilibrium, an axial force ΔN and ΔM must be applied to the section.

The change of strain due to creep and shrinkage may be considered to be artificially prevented by restraining actions of – ΔN and – ΔM. When ΔN and ΔM are applied to the section, the restraining actions are removed and equilibrium is restored. The increments of top fiber strain $\Delta\varepsilon_o$ and curvature $\Delta\kappa$ produced by the axial force *ΔN* and moment *ΔM,* gradually applied about the top reference level, may be obtained from,

$$\begin{Bmatrix} \Delta\varepsilon_o \\ \Delta k \end{Bmatrix} = \frac{1}{\overline{E}_e\left(\overline{A}_e\overline{I}_e - \overline{B}_e^{\,2}\right)}\begin{bmatrix} \overline{I}_e & \overline{B}_e \\ \overline{B}_e & \overline{A}_e \end{bmatrix}\begin{Bmatrix} \Delta N \\ \Delta M \end{Bmatrix} \quad (11)$$

where $\overline{A}_e =$ area of age adjusted transformed section

$\overline{B}_e =$ first moment of area $\overline{A}_e$ about top fiber

$\overline{I}_e =$ second moment of area $\overline{A}_e$ about top fiber

Age adjusted effective modulus $\overline{E}_e$ and corresponding modular ratio are used in these equations, since *ΔN* and *ΔM* are gradually applied. The restraining forces – *ΔN* and – *ΔM* are calculated as follows:

Creep: If creep were not restrained in any way, the top fiber strain and curvature would increase to $\phi(t,\tau_0)\varepsilon_{oi}$ and $\phi(t,\tau_0)k_i$ respectively, during the time interval (t,τ_0), where $\phi(t,\tau_0)$, ε_{oi}, and k_i are the creep coefficient, the initial strain and the initial curvature respectively. The restraining forces required to prevent this deformation are

$$-\Delta N_{creep} = -\sum_{j=1}^{n} \overline{E}_{ej}\phi_j\left(A_{cj}\varepsilon_{0i} - B_{cj}k_i\right) \quad (12)$$

$$-\Delta M_{creep} = -\sum_{j=1}^{n} \overline{E}_{ej}\phi_j\left(-B_{cj}\varepsilon_{0i} - I_{cj}k_i\right) \quad (13)$$

where A_{cj} = area of the j^{th} concrete element

B_{cj} and I_{cj} are first and second moments of the area of j^{th} concrete element about the top reference level respectively. The initial strain ε_{oi} and curvature, k_i are found from the transformed area of cross section.

Shrinkage: If the shrinkage is assumed uniform over the depth of the section and completely unrestrained, the shrinkage induced top fiber strain which develops during the time interval (t,τ_0) is $\varepsilon_{sh}(t,\tau_0)$ and curvature is zero. The restraining forces required to prevent this uniform deformation is given by

$$-\Delta N_{shrinkage} = -\sum_{j=1}^{n} \overline{E}_{ej}\left(A_{cj}\varepsilon_{shi}\right) \quad (14)$$

$$-\Delta M_{shrinkage} = +\sum_{j=1}^{n} \overline{E}_{ej}\left(B_{cj}\varepsilon_{shi}\right) \quad (15)$$

Total restraining forces and moment –ΔN, and –ΔM, which are required to prevent the free development of creep and shrinkage in each of *n* concrete element may be computed from the following equations:

$$-\Delta N = -\sum_{j=1}^{n} \overline{E}_{ej}\left[\phi_j\left(A_{cj}\varepsilon_{0i} - B_{cj}k_i\right) + \varepsilon_{shj}A_{cj}\right] \quad (16)$$

$$-\Delta M = -\sum_{j=1}^{n} \overline{E}_{ej}\left[\phi_j\left(-B_{cj}\varepsilon_{0i} + I_{cj}k_i\right) - \varepsilon_{shj}B_{cj}\right] \quad (17)$$

The change of the strain distribution with time is calculated using equation (11), and ΔN and ΔM are applied to the age-adjusted transformed section.

The age adjusted effective modulus of one of the concrete elements ($\overline{E}_{e1}$, say deck slab) is selected as the modulus of age adjusted section. The age adjusted effective modulus is calculated using the following equation:

$$\overline{E}_e(t,\tau_0) = \frac{E_c(\tau_0)}{1 + \chi(t,\tau_0)\phi(t,\tau_0)} \quad (18)$$

where $\chi(t,\tau_0)$ is the concrete aging coefficient, which accounts for the effect of aging on the ultimate value of creep for stress increments or decrements occurring gradually after the application of the initial load. The value of the aging coefficient varies between 0.6 and 1.00, and is typically about 0.8 for long time intervals. The deck is transformed into equivalent areas of the concrete of the deck slab by multiplying by the age adjusted modular ratio, $\overline{n}_{sj} = \dfrac{E_{sj}}{\overline{E}_{e1}}$

The change of stress $\Delta\sigma$, at a point in the j^{th} concrete element at a depth y below the top fiber is equal to the sum of the stress loss due to relaxation of the age-adjusted transformed section, when creep and shrinkage are fully restrained, and the stress which results when ΔN and ΔM are applied to the cross section.

$$\Delta\sigma_c = -\overline{E}_{ej}\left[\phi_j\left(\varepsilon_{0i} - yk_i\right) + \varepsilon_{shj} - \left(\Delta\varepsilon_0 - y\Delta k\right)\right] \quad (19)$$

The stress change with time in the j^{th} layer of steel is

$$\Delta\sigma_{sj} = E_{sj}\left(\Delta\varepsilon_0 - d_{sj}\Delta k\right) \quad (20)$$

Based on the principle of superposition, the total concrete strain at any time is assumed to be composed of instantaneous strain due to applied load and strains due to time effects consisting of creep and shrinkage. In addition to the time effects, if the structure is statically indeterminate, time effects cause a gradual distribution of redundant moment δM over the period the load is sustained.

Again, if the stress in the concrete at the hogging bending moment region exceeds the tensile strength of the concrete f_t', in a previously uncracked section then, concrete is no longer effective and contribution of concrete to the transformed area is ignored causing a reduction in the stiffness. Concrete stress at each time step is checked on previously uncracked sections along the length and reanalyzed when crack occurs.

TEMPERATURE EFFECTS

Thermal movements in the bridge structure significantly affect the bridge behavior. They cause serious problems, if not adequately considered in the design and maintenance of the bridges. Temperature distribution in the bridge is obtained based on three basic heat flow components, namely, radiation, convection, and conduction. The parameters that influence the temperature distribution in the bridges are cloud cover, air temperature, wind speed, the solar position angles, the orientation of the structure with respect to the sun, and the geometry and materials of the bridge. Field observations reveal that generally one-dimensional analysis is adequate for obtaining temperature distributions and the maximum bridge temperature ranges[10].

A constant temperature distribution is assumed. The horizontal displacement at each abutment due to variation in temperature is calculated as $\Delta_t = \alpha_t \Delta T L_b$, where α_t is the coefficient of thermal expansion, ΔT is the temperature range and L_b is the total length of the bridge. Fifty percent of this displacement is apportioned to each of the abutments. This horizontal displacement induces moment of $6EI\Delta_t/L^2_p$ and a horizontal force of $12EI\Delta_t/L^3_p$ on the pile head.

Stress developed in the pile due to the longitudinal displacement of the superstructure is assumed to have no significant effect on the pile capacity; however, secondary P-Δ effect is accounted for. For an equivalent cantilever with a horizontal, head displacement, Δ (Fig. 2) the combined effects of moment, M and shear, H balance the overturning moment, PΔ.

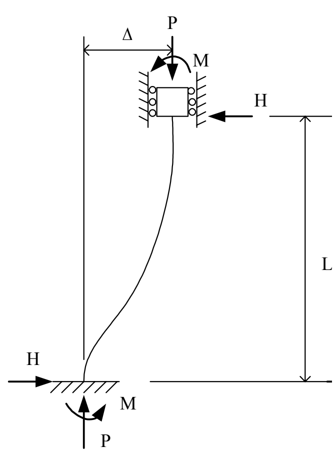

Fig. 2 Equivalent Cantilever: for a Fixed-Head Condition

TWO SPAN BRIDGE WITH RESTRAINT AT THE INTEGRAL ABUTMENTS

A two span composite steel/concrete girder is modeled as a continuous beam with fixed ends as shown in Fig 3. The reaction at the internal support and the moment at the left support are selected as redundant. Invoking the principle of virtual work, the redundant forces are determined with the conditions that the deflection at the internal support and the rotation at the left support are zero. Considering the symmetry of the structure, the total moment *M (x)* at any section at a distance *x* from left support in the left span is

$$M_x = wlx - \frac{R_c x}{2} - \frac{wx^2}{2} - M_A \qquad (21)$$

An iterative procedure is carried out using modified stiffness neglecting the contribution of concrete in the cracked region of the beam with the initial elastic solution values of R_{ci} and M_{Ai} to draw elastic moment diagram from the above equation and estimate the extent of cracking by examining the top fiber concrete stress in the hogging moment region with an assumption that initial crack occurs simultaneously at a distance *a*, from the left support as well at a distance *a1* from the internal support as shown in Fig. 3 (a).

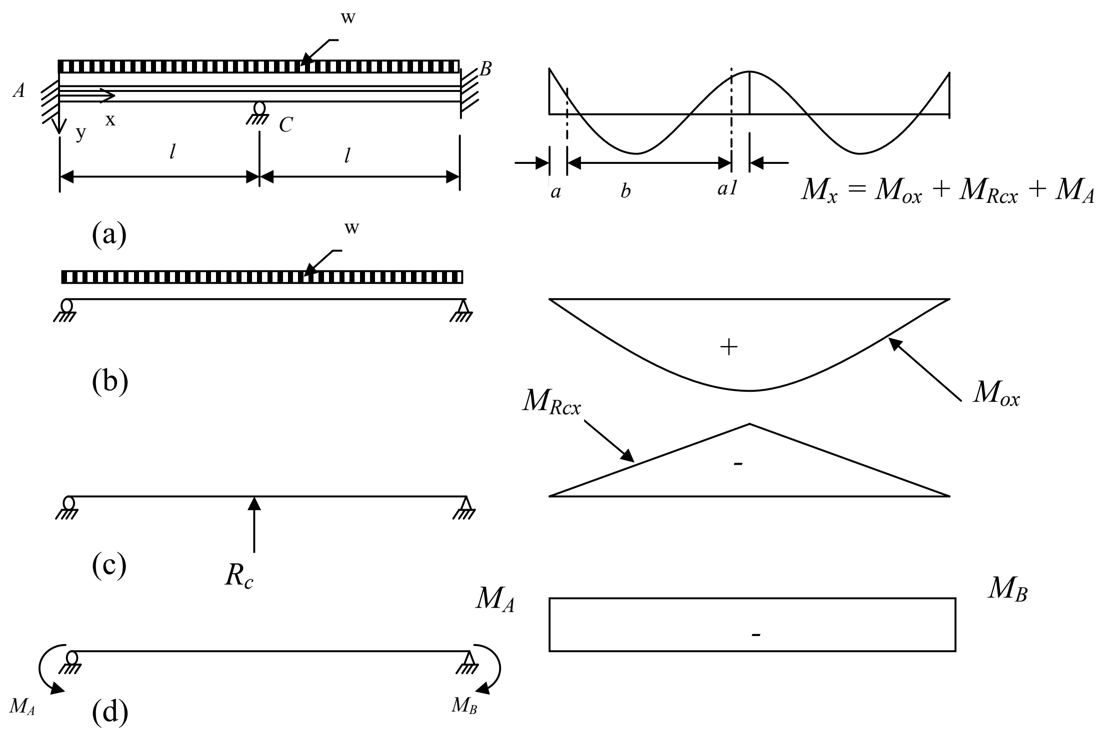

Fig. 3 Bending Moment Diagrams (a) Two Span Composite Steel/Concrete Girder; (b) Primary Released Structure; (c) Redundant Reaction at Midsupport and (d) Redundant Moments at the Supports

During the period of sustained load, the redundant reactions R_c and M_A change by an amount δR_c and δM_A thus causing a change in moment in the left span to δM_x given by

$$\delta M_x = -\frac{\delta R_c x}{2} - \delta M_A \qquad (22)$$

Adding this moment to the instantaneous moment, the change in the redundant forces δR_{ci} and δM_{Ai} may be derived again invoking the principle of virtual work using time dependent cross sectional and material properties.

Then the long term redundant R_c and M_A are

$R_c = R_{ci} + \delta R_c$ and $M_A = M_{Ai} + \delta M_A$ .... (31)

The change in moment, strain, curvature, stresses in steel and concrete on any section due to time effects may be determined from the above formulations.

TWO SPAN BRIDGE CONSIDERING FLEXIBILITY OF THE INTEGRAL ABUTMENTS

The jointless integral abutment bridges do not have an expansion joint between the abutments and the bridge superstructure; therefore, the bridge girders are rigidly connected to the foundation. The foundation consists of stub type abutment supported on single row of piles.

Changes in temperature induce movements in bridges. Bridge movements caused by this thermal expansion or contraction and creep and shrinkage of concrete induce bending stresses in the piling that supports the abutments, which must be resisted by the bridge and its substructure[11]. In jointless integral abutment bridges, the substructures must absorb the induced movements of the superstructure. The supporting foundation, therefore, has to be flexible enough to accommodate superstructure deformation due to volume changes caused by temperature, creep and shrinkage. The required flexibility is provided by the use of a stub abutment supported by a single row of piles.

A typical integral abutment bridge usually consists of abutment, wing walls and piles supporting the abutment. The abutments may be considered as rigid due to their physical configuration and restraint provided by the backfill. Thus, the abutment and backfill interaction lead to combined stiffness effects of the abutment and the backfill. The analysis of superstructure-abutment-substructure interface poses highly complex non-linear situation due to soil properties, and the material non-linearity. The joint between superstructure and substructure is modeled as discrete springs for translational and rotational degrees of freedom representing the substructure[9]. The spring stiffness for each degree of freedom of each component of the substructure may be developed by considering the resistance provided by soil to statically applied displacements of each component of substructure. In order to analyze the substructure system, the stiffness of the substructure system should be known. Fig. 4 shows discrete springs for translational and rotational degrees of freedom.

The expressions for spring stiffness[9] for the two dimensional problem are given by

$$k_{xx} = \frac{E_s B}{\left(1-\nu^2\right) I^e} + k_x^p + 2k_x^w \quad \text{(32)}$$

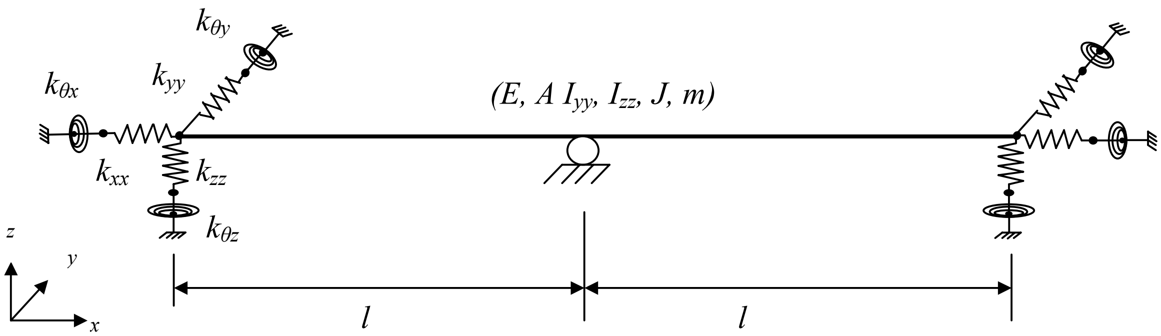

Fig. 4 Modeling of Abutment and Pile as Translational and Rotational Springs (Wilson, 1988)

$$k_{zz} = \frac{E_s B}{(1-\nu^2) I^{ef}} + \frac{2E_s W}{(1-\nu^2) I^{wf}} + k_y^p + 2k_z^w \qquad (33)$$

and

$$k_{\theta y} = \frac{E_s B}{12(1-\nu^2) H I^e}\left[\frac{D^3}{24} + \frac{1}{3}\left(H - \frac{D}{2}\right)^3\right] + \frac{2E_s W L^2}{(1-\nu^2) I^{wf}} + k_x^p \left(H - \frac{D}{2}\right)^2 + 2k_z^w L^2 \qquad (34)$$

where E_s = modulus of elasticity of the soil,
k_x^p and k_y^p = total lateral stiffness of abutment piles in the x and y directions respectively,
k_x^w and k_y^w = total lateral stiffness of wingwall piles in the x and y directions respectively,
I^e = influence factor for abutment,
I^{ef} = influence factor for pile cap,
ν = Poisson's ratio.
B = width of the abutment,
H = height of the abutment,
D = total depth of the bridge deck, and
L = length of the wingwall

The bridge structure is then analyzed by conventional structural analysis procedure considering the moments obtained from the time dependent analysis applied at the superstructure-abutment joint with the stiffness of the substructure system determined from the equations 32 – 34. Seventy five percent of the calculated moment in the abutment-pile-soil system is apportioned to the piles of the substructure system[9].

NUMERICAL ILLUSTRATION

A two span continuos concrete-steel girder integral abutment bridge shown Fig. 5 is analyzed using the above procedure. The end supports are assumed as fixed, owing to the rigidity provided by the abutment-wingwall-pile system.

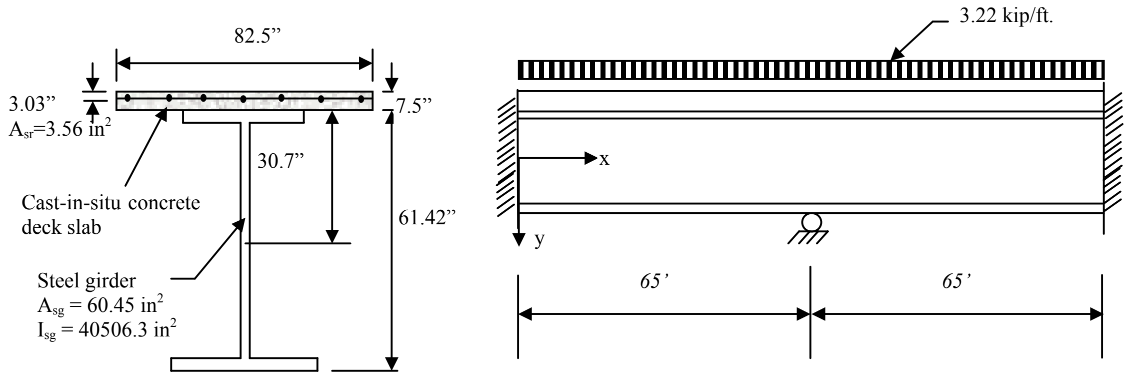

Fig. 5 Two Span Integral Abutment Bridge

SUPERSTRUCTURE ANALYSIS

The iterative procedure developed is used to analyze the time dependent bending moment along the span of the superstructure. The change in bending moment at interior support over a period of 10000 days is shown in Fig. 6 both for fixed end condition and for pinned end condition. There is considerable rate of increase in the moments in the first three months. The rate of increase in moment is insignificant after about six months in the integral abutment bridge with fixed ends. However, the rate of moment increase is insignificant after about one year in the case of integral abutment bridges with pinned end supports. The computed instantaneous moment and time dependent bending moment due to creep and shrinkage effects up to one year time period for fixed end condition is shown in Fig. 7(a). Moments for a two span continuous composite bridge structure with simple supports are plotted in Fig. 7(b). There is a rapid increase in the moment along the span in the first two months period due to creep and shrinkage effects. The rate of change in moment decreases after this period. The moment value reaches a near constant value in one year. It can be seen from the resulting time dependent bending moment diagrams, that assumption of a simple support at the ends for an integral abutment bridge produces approximately twice the moment in the girder with fixed end condition.

SUBSTRUCTURE ANALYSIS

It is assumed that medium dense sand having a soil modulus of 360 ksf is used as backfill in the abutment. The influence factors I^e and I^{ef} are assumed as 2.0, which usually vary from 1.0 to 3.0. A value of 0.3 is assumed for Poisson's ratio. The width of the abutment wall is assumed as 45.1 ft. Equivalent cantilever length based on stiffness criterion[12] is used to evaluate the stiffness of the pile. The stiffness of the substructure system is determined from the equations 32-34. The bridge system shown in Fig. 4 is then analyzed by conventional structural analysis procedure considering the moments obtained from the time dependent analysis applied at the superstructure-abutment joint. Seventy five percent of

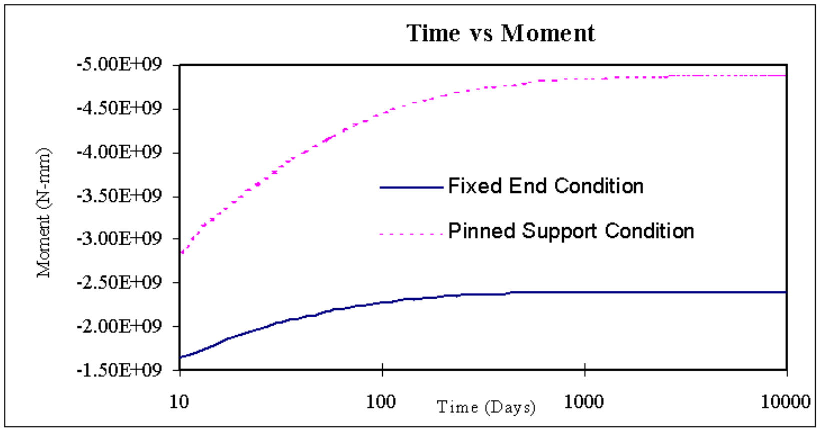

Fig. 6 Change in Bending Moments at Interior Support with respect to Time

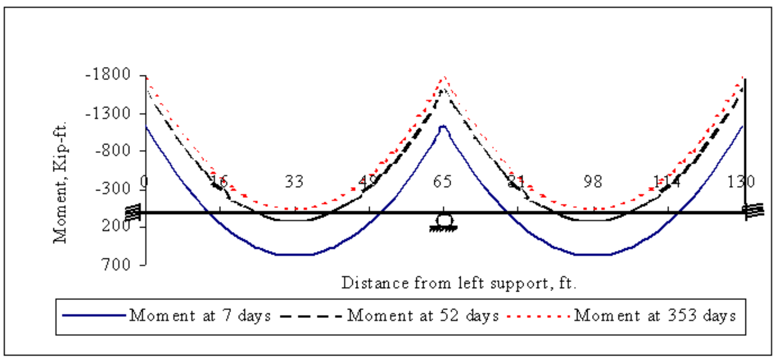

(a)

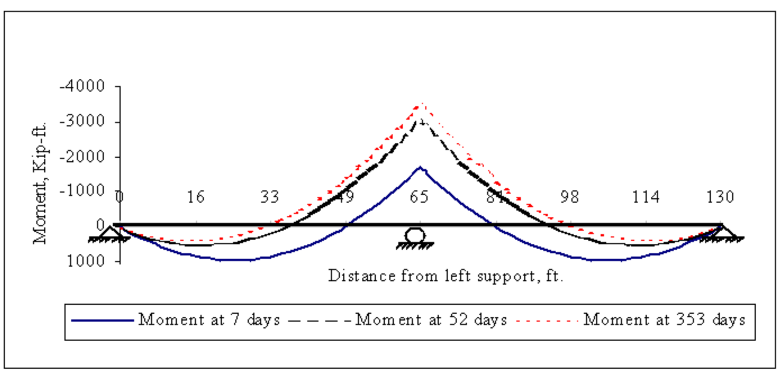

(b)

Fig. 7 Time Dependent Bending Moment diagrams: (a) Fixed End Condition; (b) Pinned Support Condition the calculated moment in the abutment-pile-soil system is apportioned to the piles supporting the abutment.

The pile is then analyzed for the lateral deflection, bending moment, shear force and stress along the depth. The results of the analysis are plotted in Fig. 8 (a) – (d).

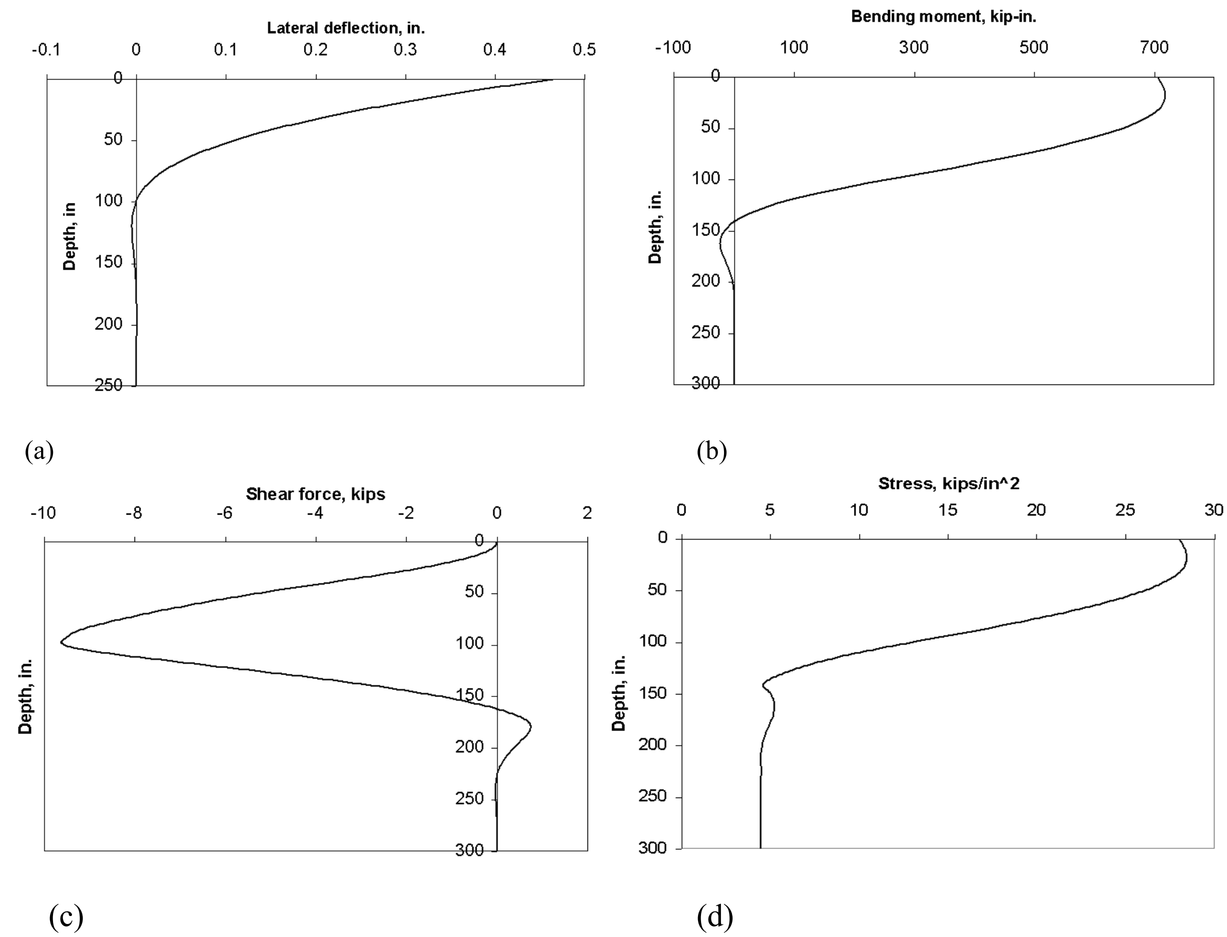

Fig. 8 Pile Analysis Results along the Depth: (a) Variation of Horizontal Displacement; (b) Variation of Bending Moment; (c) Variation of Shear; (d) Variation of Stress

The pile analysis shows that the pile lateral displacement of 0.5 in. and the stress in the pile are within the allowable limits. The lateral displacement, moment, shear and stress obtained by this approach are comparable to those of the values obtained using secondary P-Δ method for laterally loaded piles[13].

CONCLUSIONS

A computer model for calculating the time-dependent behavior due to creep and shrinkage of continuous steel-concrete composite deck integral abutment bridge has been developed and illustrated with a numerical example. Creep and shrinkage are evaluated using the ACI model. Age-adjusted effective modulus approach is used to determine time dependent cross sectional properties. Variation in the material properties across the depth of the section is modeled considering the transformed area of cross section. Material nonlinearity introduced by cracking in the slab in the negative moment region is accounted for along with the time dependent deformations caused by creep and shrinkage in the concrete.

The partial rigidity provided by the integral abutment and the sub-structure system is incorporated by modeling the composite girder with fixed end supports. Time dependent bending moment of the composite steel girder/concrete slab system is determined and presented based on the creep and shrinkage effects.

There is a rapid increase in the bending moment in the initial period of two months due to creep and shrinkage effects. The moment reaches almost a constant value in about one year. Hence, there is little need for long-term time dependent analysis of more than one year. From the resulting time dependent bending moment diagrams, the assumption of a simple support for an integral bridge superstructure produces almost twice the moment in the girder with fixed end condition. Comparison of results obtained from the analysis assuming the composite steel girder/concrete slab system as a continuous beam with simple supports and as a continuous fixed beam shows that for efficient system response, partial rigidity provided by the substructure system should be included in the analysis of integral abutment bridges.

The partial restraint provided by the abutment-pile-soil system to the superstructure is considered in the analysis based on modeling using discrete spring stiffness values for translation and rotation. The analysis shows that the pile could accommodate reasonable lateral displacement without exceeding the allowable stress in the pile section, which is comparable to the values, obtained using secondary P-Δ method for laterally loaded piles.

ACKNOWLEDGEMENT

The authors wish to express sincere thanks to Florida Department of Transportation (FDOT) for the financial support of the study presented in this paper (research project: Design Consideration for Integral Abutment Bridges in Florida, Contract No. BC342), Principal investigator: Dr M. Arockiasamy, Project Manager: Marc Ansley). They wish to express their appreciation to Dr S. Nix, Professor and Chairman, Department of Civil Engineering, and Dr Karl K. Stevens, Dean, College of Engineering, Florida Atlantic University for their continued interest and encouragement.

REFERENCES

1. Kunin, J., and Alampalli, S., "Integral Abutment Bridges: Current Practice in United States and Canada", *Journal of Performance of Constructed Facilities*, Vol. 14, No. 3, August 2000, pp.104-111.
2. Wolde-Tinsae, A. M., and Greimann, L. F., "General Design Details for Integral Abutment Bridges", *Journal of Boston society of Civil Engineers*, Vol. 3, No. 2, Fall 1988, pp. 7-20.
3. Wasserman, E. P., "Tennessee State Route 50 Bridge Over Happy Hollow Creek", *PCI Journal*, September-October 1999, 26-36.
4. Burke, M. P, Jr., "Integral Bridges", *Transportation Research Record*, No. 1275, 1990, pp. 53-61.
5. Gilbert, R. I., and Bradford, M. K., "Time-Dependent Behavior of Continuous Composite Beams at Service Loads", *Journal of Structural Engineering*, Vol. 121, No. 2, February 1995, pp. 319-327.
6. Kwak, H. G., and Seo, Y. J., "Long-term Behavior of Composite Girder Bridges", *Computers and Structures*, Vol. 74, 2000, pp. 583-599.
7. Destrebecq, J. F., and Jurkiewiez, B., "A Numerical Method for the Analysis of Rheologic Effects in Concrete Bridges, *Computer Aided Civil and Infrastructure Engineering*, Vol. 16, 2001, pp. 347-364.
8. Thippeswamy, H. K., and GangaRao, H. V. S., "Analysis of In-Service Jointless Bridges", *Transportation Research Record*, No. 1476, 1996, pp. 162-170.
9. Wilson, J. C., "Stiffness of Non-skew Monolithic Bridge Abutments for Seismic Analysis", *Earthquake Engineering and Structural Dynamics*, Vol. 16, 1988, pp. 867-883.
10. Moorty, S., and Roeder, C. W., "Temperature Dependent Bridge Movement", *Journal of Structural Engineering*, Vol. 118, No.4, April 1992, pp. 1090-1105.
11. Abendorth, R. E., and Greimann, L. F., "Abutment Pile Design for Jointless Bridges", *Journal of Structural Engineering*, Vol. 115, No. 11, November 1989, pp. 2914-2929.
12. Greimann, L. F., Abendroth, R. E., Johnson, D. E., and Ebner, P. B., "Pile Design and Tests for Integral Abutment Bridges", *Final Report, IOWA DOT Project HR-273*, December 1987, p. 302.
13. Arockiasamy, M., Butrieng, N., and Sivakumar, M., "State-of-the-art of Integral Abutment Bridges: Design and Practice", accepted for possible publication in the *Journal of Bridge Engineering*, May 2002.